International Journal of Thin Films Science and Technology

http://dx.doi.org/10.18576/ijtfst/100303

Effect of Implantation Time of Cupper Nitride onto ITO Thin Films: Structural, Morphological, Electrical, and Optical Properties

A.M. Hassan , E.F. Kotp and E.R. Shaaban[*]

Physics Department, Faculty of Science, Al-Azhar University, Assiut 71524, Egypt.

Received: 16 Jul. 2021, Revised: 13 Aug. 2021, Accepted: 23 Aug. 2021.
Published online: 1 Sep. 2021.

Abstract: Copper nitride (Cu_3N) thin films have been implanted onto an electron beam evaporated films of indium tin oxide (ITO) from Cu metal target using reactive dc Magnetron Sputtering (dcMS) technique in a nitrogen/argon atmosphere at room temperature. The implantation parameter was kept constant excepting the implantation time. The effect of implantation time upon microstructural, morphological, electrical, and optical properties have been studied. The elemental composition of the as-deposited and Cu_3N implanted has been studied by using the EDXS technique, and the spectrum shows peaks belonging to In, Sn, O, Cu, and N. A zinc blend structure was observed for all the investigated films with no sign of impurities. The optical direct energy bandgap E_g^{opt} is found to decreases from 3.49 eV to 2.62 eV with increasing the implantation time of Cu_3N. The refractive index *n* is increased with increasing the exposure time of implantation. The refractive index has abnormal behavior in the infrared region due to the strong absorption in this region that appears in transmission spectra. The electrical resistivity decreases from 1908.22 Ω.cm to 165.24 Ω.cm with increasing the duration time of implantation.

Keywords: Reactive magnetron sputtering; ITO substrates; Cu_3N thin films; Microstructural properties; Optical properties, Electrical properties.

1 Introduction

Transparent conducting oxides (TCO) have a broad range of physical properties that make them ideal for several applications such as optoelectronic devices, antireflection coatings, transparent electrodes in solar cells, and heat-reflecting mirrors in glass windows, and many others [1]. Indium tin oxides (ITO) are widely used in optoelectronic applications as transparent conductive electrodes (TCE) for light-emitting and light detecting devices. This is due to its unique properties of highly transparent over the visible spectrum (>80%), very low resistivity ($\sim 10^{-4}$ Ω cm), high carrier concentration ($\sim 10^{21} cm^{-3}$) with mobility around 10–30 cm^2/Vs, wide optical band gap(~3.6–4 eV) and high work functions (~4.20 eV) [2-6]. ITO is considered one of TCO. [7]. Besides, ITO reveals interesting and technological significance in window coatings, solar cells, flat panel displays, and energy-saving buildings [8]. The structural, electrical, and optical properties of ITO films such as morphology, energy gap, and impurity type are strongly governed to a large extend by the preparation and growth conditions [9-11]. Furthermore, due to the various deposition parameters, films deposited by any process can have a wide range of characteristics. As a consequence, manipulating the deposition parameters will alter the film's properties.

Transition metal nitrides show a wide variety of physical properties and applications. In the 3d transition metals (Ti, Cr, Fe, Co, Ni, and Cu) the reactivity with nitrogen decreases as the atomic number increases [12]. Copper nitrides Cu_3N have gained significant interest as a new material for optical storage devices and integrated high-speed circuits, based on their specific properties, such as the very low temperature of thermal decomposition, excellent electrical properties, and optical qualities [13]. The crystal structure of Cu3N is one of the anti-ReO_3 types with a simple cubic unit cell of lattice constant (a = b = c =

[*]Corresponding author E-mail: esam_ramadan2008@yahoo.com

3.817 Å, and α = β = γ = 90°) [14, 15]. Until now, many deposition methods have been used to prepare Cu3N films, such as beam epitaxy [16], atomic layer deposition [17], pulsed laser deposition [18, 19], dc-triode sputtering [20, 21], and mostly, reactive magnetron sputtering [22-27].

It is well known that the properties of ITO films are significantly controlled by the type of growth method. Recently, a lot of different growth techniques have been used; such as pulsed laser ablation (PLD) [28], electron beam evaporation [29], chemical vapor deposition [30], ion beam assisted deposition (ISD) [31], dip coating [32], ion embedding [33] and RF magnetron sputtering [34, 35]. Many preparation parameters were used to improve the crystallinity of films including growth temperature; film thickness, post-annealing temperature, and dc or RF power [36]. Generally, the implantation process can be used to improve material properties [37-39]. Thus, this paper aims to prepare high-quality ITO films by using the electron beam deposition technique after that, implantation of Cu_3N onto those films by using reactive sputtering, and studying the effects of the implantation time on the structural, optical, and electrical properties of the ITO films for solar cells.

2 Materials and Methods

2.1 ITO Ingot Target Preparations

Indium tin oxide ingot target was prepared by a conventional solid-state reaction method in air. High purity In_2O_3 (99.99%) and SnO_2 (99.999%) analytical grade powders (Aldrich) in stoichiometric quantities of 95 wt. % In_2O_3 and 5 wt. % SnO_2 are mixed in a ball mill for about one hour. The mixed powder is then compressed into a disc-shaped pellet by using uniaxial compression at 210 MPa. The pellets were sintered at 1200 °C at a rate of 20°C/min in an ambient atmosphere and then cooled to room temperature at a rate of 20 °C/min.

2.2 Thin Films Deposition

Electron beam evaporation technique (type; Denton Vacuum DV 502 A) is used to prepare ITO thin films from the obtained ingot target on a glass substrate with a thickness of 100 nm. The substrates were carefully cleaned in the following steps: 15 minutes in acetone, 15 minutes in distilled water, 10 minutes in ethyl alcohol, and 15 minutes ultrasonically washing in deionized water. The substrates were dried using nitrogen gas. At a pressure of 5 × 10^{-5} Torr, the ITO pellet and substrates were then inserted into the vacuum chamber. To outgas the target and remove any pollutants, the ITO pellet target was preheated for 5 minutes before the deposition. The substrates were placed 20 cm away from the ITO powder target at room temperature. The deposition rate was of 2 nm/sec. The thickness and rate of evaporation of the films were observed by using a thickness monitor (quartz crystal monitor DTM 100). After that, the coated films treated with reactive dcMS system (Denton Vacuum DV-502A with DSM-300A external sputter head mounted on top of a bill gar with a maximum power of 300 W and it is protected by a cylindrical aluminum guard) to implantation Cu_3N the thin films using high purity copper metal target purity of 99.9%, 1016 mm in diameter and 5 mm in thickness, onto ITO coated films (see Fig. 1). To obtain the uniform film a mechanical rotation of the substrate holder (≈ 40 rpm) during implantation was used.

The gas flows controlled with a flow meter as a gas flow rate of the gas mixture and the gas pressure was monitored by Pirani Penning gauge with Edward's controller 1005. The high vacuum inside the chamber was 10^{-5} Torr, using rotary and diffusion pumps, the working gas pressure was 30 mTorr, and the duration time during implantation was 0.0, 5.0, 10, 15, 20, and 25 minutes.

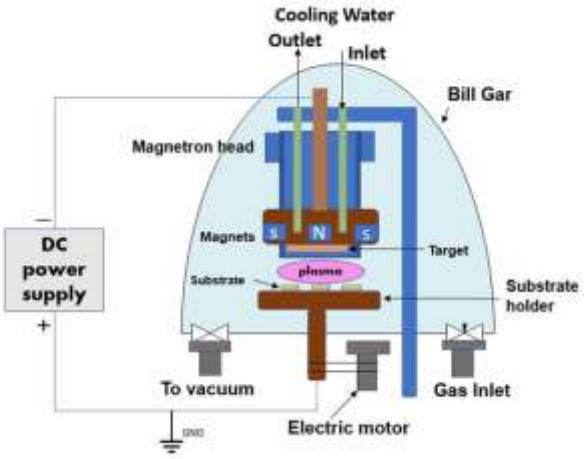

Fig. 1: Schematic diagram of the dc magnetron sputtering system.

3 Results and Discussion

3.1 Structural and Microstructure Studies

3.1.1 EDXS Analysis

The elemental composition of the as-deposited and Cu_3N implanted films has been studied by using the EDXS technique. The EDXS spectrum is presented in **Error! Reference source not found.**

The spectrum in **Error! Reference source not found.** (a) shows three peaks belonging to In, Sn, and O which indicates that the Sn ions have successfully incorporated into the In_2O_3 lattice, while **Error! Reference source not found.** (b, c, and d) show the peaks belonging to N and Cu which indicates that the Cu_3N has successfully incorporated into the ITO substrate with different ratio.

3.1.2 X-ray Diffraction

The crystal structures of the as-deposited and implanted films were analyzed with Cu Ka radiation using grazing angle X-ray diffraction (D8 advance model by Brucker Company).

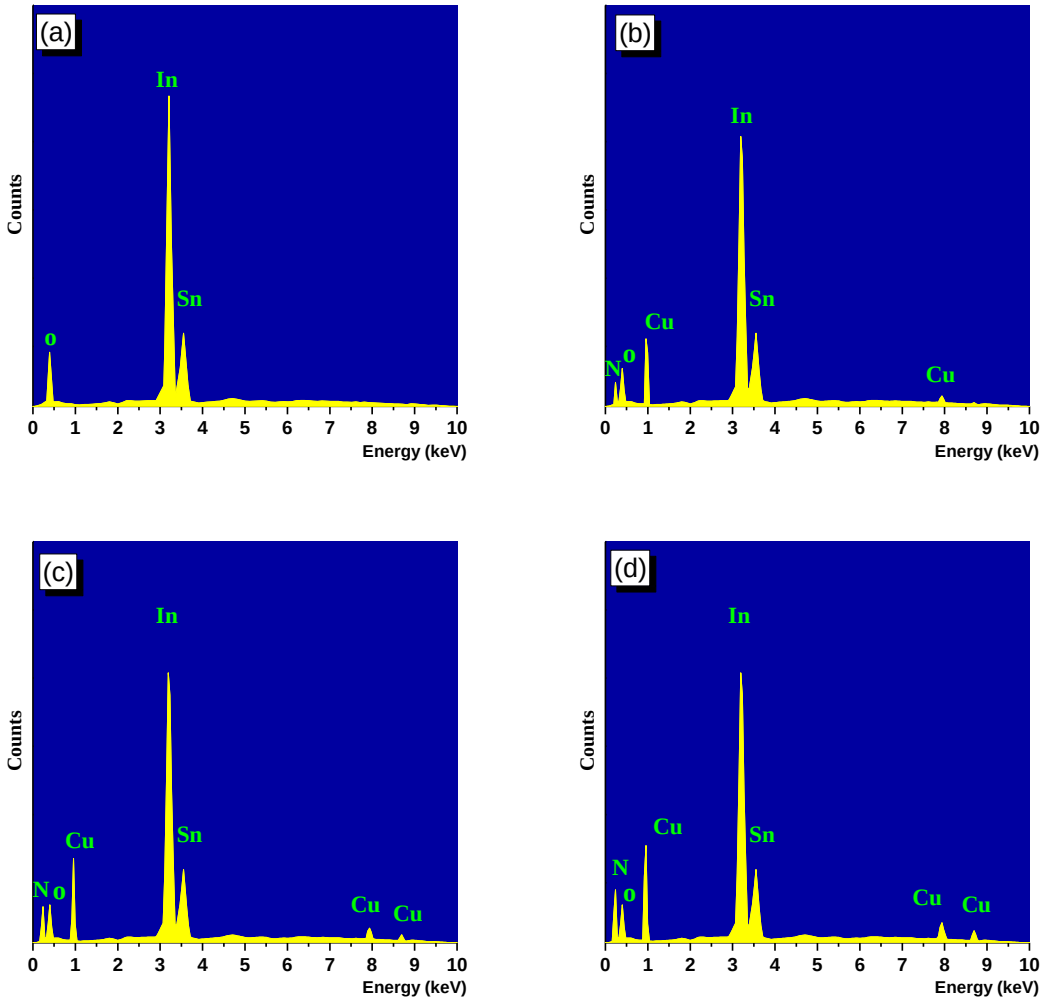

Fig. 2: EDAX of ITO as-deposited and ITO implanted by Cu_3N at (a) 0.0 min. (b) 5.0 min. (c) 15 min. and (d) 25 min.

Fig. 3 presents the XRD diagrams of the electron beam evaporated ITO and the implanted Cu_3N films at different implantation times. The as-deposited ITO film shows diffraction peaks from (222), (320), (400), and (441), planes, indicating the film is polycrystalline, while the ITO implanted films with Cu_3N show diffraction peaks from (111) and (211) with addition to those appears in ITO without implantation, and the films also are polycrystalline.

The observed diffraction lines were matched with the standard diffraction data of the Indium Tin Oxide cubic structure. Additionally, the results confirmed that the absence of any other reflection line belongs to impurities of oxide phase and/or metal clusters, which supports the integration of Sn^{+4} atoms in the In^{3+} sublattice and confirms the formation of a pure cubic phase of the implanted ITO

films without any structural transformation. Furthermore, it was found that as the implantation time increased, the intensity of the reflection line related to the (222) plane increased, which is ascribed to improve in the crystallinity of the deposited ITO thin films because the implantation treatment helps to rearrange atoms and remove the defect density in the film.

3.2 Optical Properties

It is well known that the optical parameters of semiconductors are considered to be the most essential parameters, thus, the optical properties of the ITO implanted films are presented and discussed in the following section.

3.2.1 The Measurements of Transmittance and Reflectance

with a thickness of 150 nm in the wavelength range of 300 to 2500 nm.

The results indicate that the transmittance is comparatively

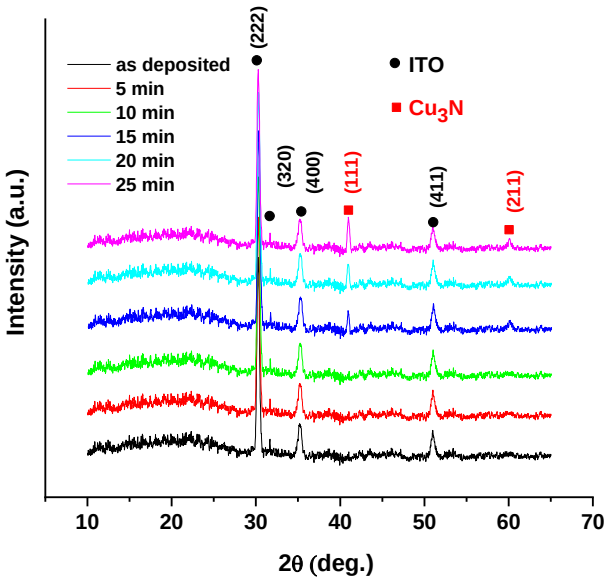

Fig. 3: XRD patterns of ITO thin films at the various implantation time of Cu_3N.

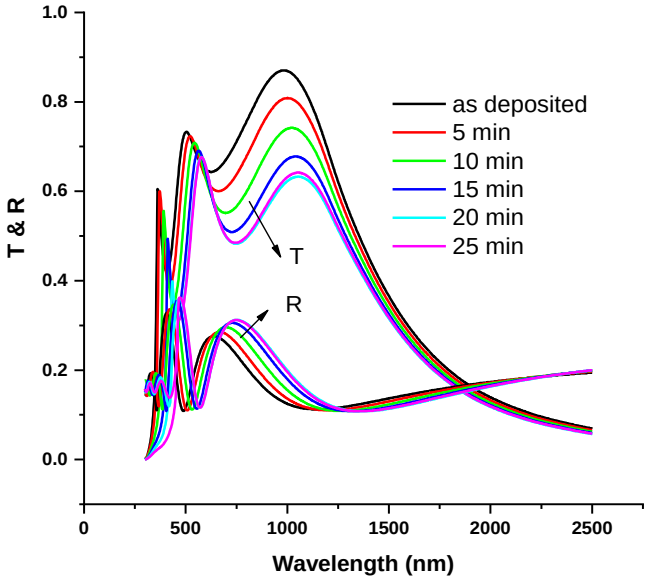

Fig. 4: The spectral variation of the absolute value of T(λ) and R(λ) of as-deposited ITO film and implanted films at different implantation times.

Fig. 4 shows the measurement results of the transmittance *(T)* and reflectance *(R)* of the as-deposited ITO film and at the implanted films at different implantation times of Cu_3N decreased for the implanted films relative to the as-deposited film. It has been found that the transmittance value decreases from 70% for the as-deposited film to 50%

for the implanted film at 25 min, thereby revealing a film with high transparency, which is beneficial for optical device applications [39-41]. Different groups have also reported similar behavior [37, 42-44]. The increment in the transmittance is due to the increase in the crystallinity of the film, where the enhancement in the crystallinity tends to reduce light scattering and defects, as reported by other researchers [45, 46]. It was observed that by enhancing the implantation treatment of the ITO film, a significant shift (redshift) of the fundamental transmittance edge to higher wavelengths can be remarked, which indicates that the energy gap increases when the implantation time increase to 25 min.

3.2.2 Absorption Coefficient and Optical Energy Band Gap Studies

The inter-band transitions and optical energy gap of semiconductors are mainly determined from the absorption coefficient. Consequently, the transmission and reflection measurements of the as-grown and implanted films are used to calculate the absorption coefficient (α) by the relation [47]:

$$\alpha = \frac{1}{d} ln \left[\frac{(1-R)^2 + [(1-R)^4 + 4R^2T^2]^{1/2}}{2T} \right] \quad (1)$$

where d is defined as the thickness of the implanted films. Fig. 5 demonstrates the wavelength-dependent absorption coefficient measurement of as-grown and implanted ITO films. It is found that three absorption coefficient regions are observed; absorption in the NIR range, transparent region, and strong absorption region in the UV range. The absorption coefficient decreases as the implantation time increases in the near IR and strong absorption regions. The latter regime is used to determine the energy gap, where a prominent reduction in the absorption curves is obtained due to the electron excitation from the VB to CB.

Furthermore, using Tauc's model to fit the results of optical measurement of as-deposited and the implanted ITO film, the optical energy gap, E_g, can be evaluated [48]:

$$\alpha h\nu = \alpha_0 (h\nu - E_g)^c \quad (2)$$

Where α_o α, c, and $h\nu$, are the Tauc parameter (dependent on the transition types), the absorption coefficient, index (referring to optical transition type), and the photon energy of incident light, respectively. Taking into account the direct allowable transition type between the bands of c=1/2, the extrapolation of the linear part of the dependence of $(\alpha h\nu)^2$ on photon energy $(h\nu)$ is used to determine the E_g^{opt} from the intercept of the extrapolated line to $(\alpha h\nu)^2 = 0$. As the implantation time increases, E_g^{opt} decreases from 3.49 eV to 2.62 eV, this can be ascribed to the decrease in crystallinity and the crystallite size of the films, which leads to an increasing in defects. According to the Davis Mott model, defects will generate localized states in the bandgap [49].

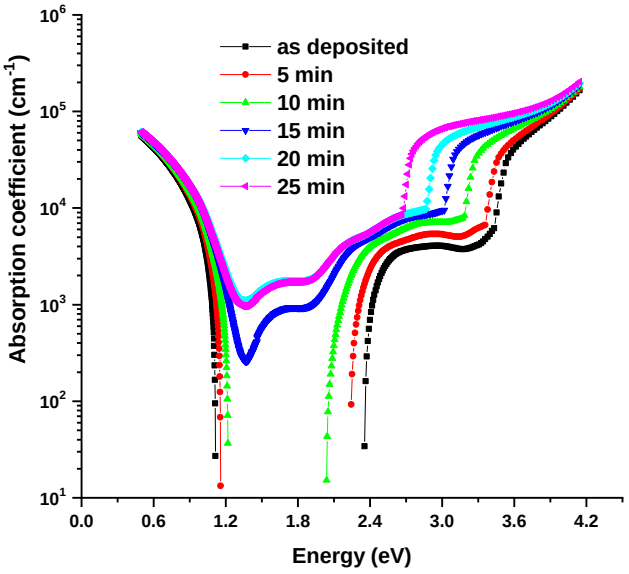

Fig. 5: The variation of absorption coefficient versus the energy for the as-deposited ITO film and implanted films at different implantation times of Cu_3N.

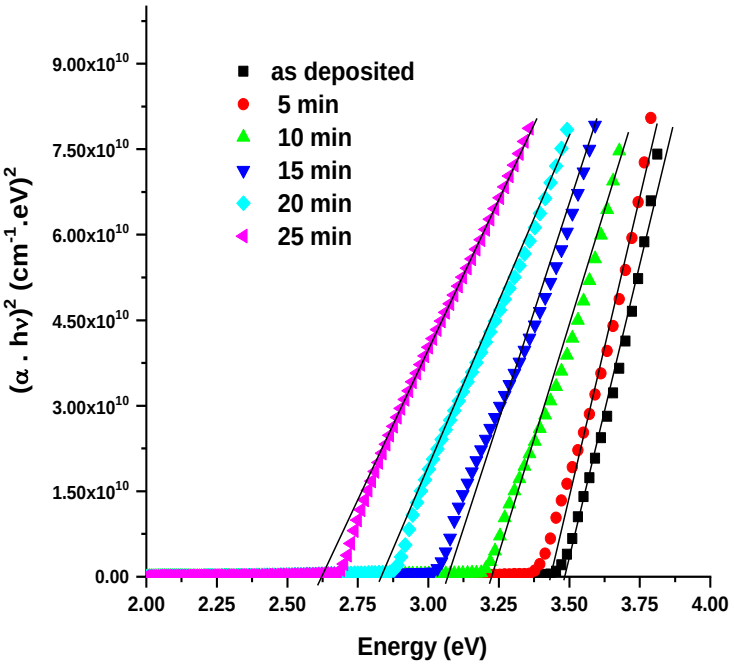

Fig. 6: A plot of $(\alpha h\nu)^2$ versus the energy ($h\nu$) for the as-deposited ITO film and the implanted films at different implantation times of Cu_3N.

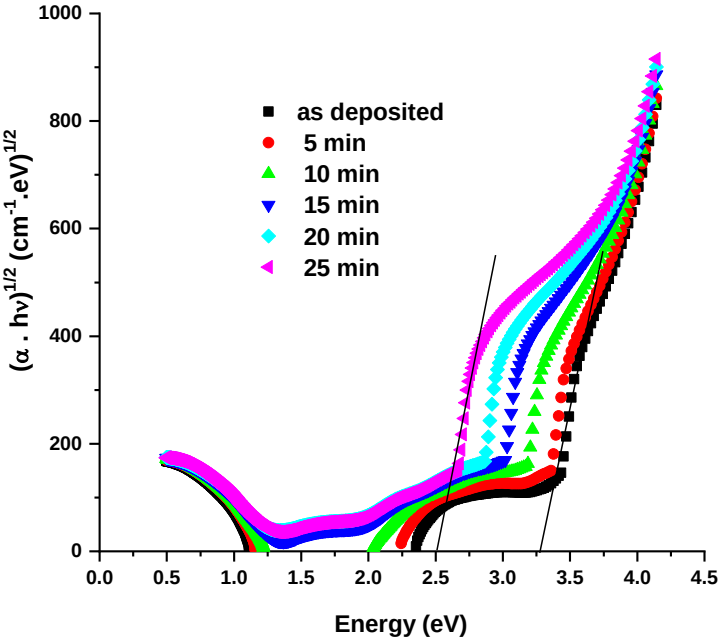

Fig.7: A plot of $(\alpha h\nu)^{1/2}$ versus the energy ($h\nu$) for the as-deposited ITO film and the implanted films at different implantation times of Cu_3N.

3.2.3 Optical Constants Determination

The refractive index (*n)* and extinction coefficient *k* ($k = \frac{4\pi\alpha}{\lambda}$), the so-called optical constants, are estimated according to the light reflection theory in which the reflectively of the film is represented in terms of Fresnel's coefficient [50]:

$$R = [(n-1)^2 + k^2] / [(n+1)^2 + k^2] \quad (3)$$

Fig. 8 shows the spectral behavior of the refractive index of as-deposited ITO and implanted films. It is found that the refractive index *n* is increased with increasing the exposure time of implantation. The refractive index has abnormal behavior in the infrared region due to the strong absorption in this region that appears in transmission spectra.

3 Electrical Studies

Fig. 9 illustrates the electrical resistivity for the as-deposited ITO film and implanted films at different implantation times of Cu_3N. The electrical resistivity of as-deposited and implanted ITO films found to be reduced from 1908.22 Ω.cm to 165.24 Ω.cm with increasing the duration time of implantation. This remarked reduction in electrical resistivity is ascribed to the improvement of the film crystallinity and the increase of the film grain size. These results are in agreement with those reported in the kinds of literature [51, 52].

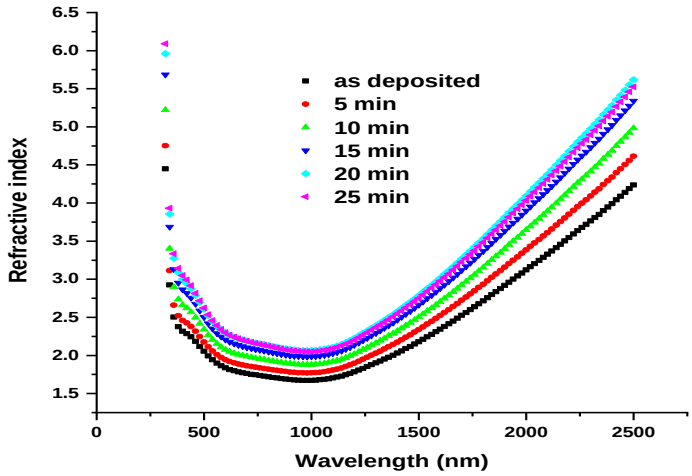

Fig. 8: The spectral variation of the refractive index of as-deposited ITO film and implanted films at different implantation times of Cu_3N.

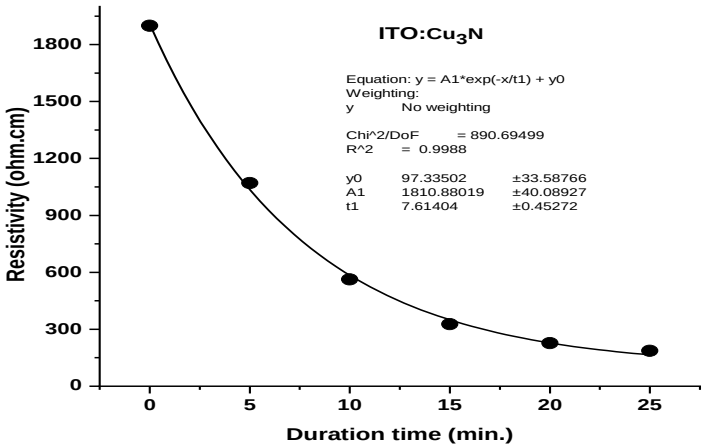

Fig. 9: The variation of electrical resistivity of ITO film with the duration time of implantation Cu_3N.

4 Conclusions

In summary, ITO thin films were fabricated by electron beam evaporation onto clean glass substrates. The Cu_3N was implanted by reactive dc magnetron sputtering on the surface of the ITO films. The effect of implantation time upon microstructural, morphological, optical, and electrical properties was investigated. A zinc blend structure was observed for all the investigated films with no impurity phase appears in the XRD pattern. The elemental composition spectrum of the as-deposited and Cu_3N implanted films shows peaks belonging to In, Sn, O, Cu, and N. The optical direct energy bandgap E_g^{opt} is found to decreases from 3.49 eV to 2.62 eV with increasing the implantation time of Cu_3N. The refractive index n has a normal dispersion from the lower wavelength till λ = 1050 nm and an abnormal trend at higher wavelengths due to strong absorption in the NIR region. The electrical measurements show that as the implantation time increases to 25 min, the electrical resistivity decreases from 1908.22 Ω.cm to 165.24 Ω.cm, which is ascribed to the improvement of the film crystallinity and the increase of the grain size. The tunability for both optical properties represented with (n, E_g^{opt}) and electrical properties represented with resistivity ρ recommend the implanted ITO thin films with CU3N for solar cells and optoelectronic devices.

References

[1] Lewis, B.G. and D.C.J.M.b. Paine, Applications and processing of transparent conducting oxides. MRS Bulletin., **25(8)**, 22-27, 2000.

[2] Isiyaku, A.K., A.H. Ali, and N. Nayan, Structural optical and electrical properties of a transparent conductive ITO/Al-Ag/ITO multilayer contact. Beilstein J Nanotechnol., **11(1)**, 695-702, 2020.

[3] Zhang, W., et al., Structural, electrical and optical properties of indium tin oxide thin films prepared by RF sputtering using different density ceramic targets. Vacuum., **86(8)**, 1045-1047, 2000.

[4] Schlaf, R., H. Murata, and Z.H. Kafafi, Work function measurements on indium tin oxide films. Journal of Electron Spectroscopy and Related Phenomena., **120(1)**, 149-154, 2001.

[5] Meng, L.-j. and M.P. dos Santos, Properties of indium tin oxide films prepared by rf reactive magnetron sputtering at different substrate temperature. Thin Solid Films., **322(1)**, 56-62, 1998

[6] Ali, A.H., A. Shuhaimi, and Z. Hassan, Structural, optical and electrical characterization of ITO, ITO/Ag and ITO/Ni transparent conductive electrodes. Applied Surface Science,., 288, 599-603, 2014.

[7] Ren, B., et al., Preparation and characteristics of indium tin oxide (ITO) thin films at low temperature by r.f. magnetron sputtering. Rare Metals, 2006. 25(6, Supplement 1), 137-140, 2006.

[8] Nisha, M., et al., Effect of substrate temperature on the growth of ITO thin films. Applied Surface Science., **252(5)**, 1430-1435, 2005.

[9] Reddy, V.S., et al., The effect of substrate temperature on the properties of ITO thin films for OLED applications. Semiconductor Science and Technology., **21(12)**, 1747-1752, 2006.

[10] El Akkad, F., et al., Effect of Substrate Temperature on the Structural, Electrical and Optical Properties of ITO Films Prepared by RF Magnetron Sputtering. physica status solidi (a)., **177(2)**, 445-452, 2000.

[11] Wohlmuth, W. and I. Adesida, Properties of R.F. magnetron sputtered cadmium–tin–oxide and indium–tin–oxide thin films. Thin Solid Films., **479(1)**, 223-231, 2005.

[12] Wang, J., et al., Copper nitride (Cu3N) thin films deposited by RF magnetron sputtering. Journal of Crystal Growth., **286(2)**, 407-412, 2006.

[13] Zhang, G., et al., Structure and thermal stability of copper nitride thin films. 2013. 2013.

[14] Hojabri, A., et al. The effect of nitrogen plasma on copper thin film deposited by DC magnetron sputtering. in IOP Conference Series: Materials Science and Engineering. 2010. IOP Publishing.

[15] Chen, S.-C., et al., Optoelectronic properties of Cu3N thin films deposited by reactive magnetron sputtering and its diode rectification characteristics. Journal of Alloys and Compounds., **789**, 428-434, 2019.

[16] Navío, C., et al., Intrinsic surface band bending inCu3N(100)ultrathin films. Physical Review B., **76(8)**, 085105.

[17] Törndahl, T., Atomic layer deposition of copper, copper (I) oxide and copper (I) nitride on oxide substrates. 2004, Acta Universitatis Upsaliensis.

[18] Gallardo-Vega, C. and W. de la Cruz, Study of the structure and electrical properties of the copper nitride thin films deposited by pulsed laser deposition. Applied Surface Science., **252(22)**, 8001-8004, 2006.

[19] Soto, G., J.A. Díaz, and W. de la Cruz, Copper nitride films produced by reactive pulsed laser deposition. Materials Letters., **57(26)**, 4130-4133, 2003.

[20] Gordillo, N., et al., DC triode sputtering deposition and characterization of N-rich copper nitride thin films: Role of chemical composition. Journal of Crystal Growth., **310(19)**, 4362-4367, 2008.

[21] Venkata Subba Reddy, K., et al., Copper nitride films deposited by dc reactive magnetron sputtering. Journal of Materials Science: Materials in Electronics., **18(10)**, 1003-1008, 2007.

[22] Odeh, I.M., Fabrication and optical constants of amorphous copper nitride thin films prepared by ion beam assisted dc magnetron reactive sputtering. Journal of Alloys and Compounds., **454(1)**, 102-105, 2008.

[23] Du, Y., et al., Electrical conductivity and photoreflectance of nanocrystalline copper nitride thin films deposited at low temperature. Journal of Crystal Growth.,. **280(3)**, 490-494, 2005.

[24] Liu, Z.Q., et al., Thermal stability of copper nitride films prepared by rf magnetron sputtering. Thin Solid Films., **325(1)**, 55-59, 1998.

[25] Maya, L., Deposition of crystalline binary nitride films of tin, copper, and nickel by reactive sputtering. Journal of Vacuum Science & Technology A: Vacuum, Surfaces, and Films., **11(3)**, 604-608, 1993.

[26] Nosaka, T., et al., Copper nitride thin films prepared by reactive radio-frequency magnetron sputtering. Thin Solid Films., **348(1)**, 8-13, 1999.

[27] Yue, G.H., et al., Copper nitride thin film prepared by reactive radio-frequency magnetron sputtering. Journal of Applied Physics, 2005. 98(10): p. 103506.

[28] Adurodija, F.O., et al., Highly conducting indium tin oxide (ITO) thin films deposited by pulsed laser ablation. Thin Solid Films., **350(1)**, 79-84, 1999.

[29] Matsuo, J., et al., O2 cluster ion-assisted deposition for tin-doped indium oxide films. Nuclear Instruments and Methods in Physics Research Section B: Beam Interactions with Materials and Atoms., **161-163**, 952-957, 2000.

[30] Park, Y.-C., et al., ITO thin films deposited at different oxygen flow rates on Si(100) using the PEMOCVD method. Surface and Coatings Technology., 161(1), 62-69, 2002.

[31] Yang, Y., et al., High-Performance Organic Light-Emitting Diodes Using ITO Anodes Grown on Plastic by Room-Temperature Ion-Assisted Deposition. Advanced Materials., 16(4), 321-324, 2004.

[32] Nishio, K., T. Sei, and T. Tsuchiya, Preparation and electrical properties of ITO thin films by dip-coating process. Journal of Materials Science., **31(7)**, 1761-1766, 1996.

[33] Sawada, M. and M. Higuchi, Electrical properties of ITO films prepared by tin ion implantation in In2O3 film. Thin Solid Films., **317(1)**, 157-160, 1998.

[34] Ahmed, N.M., et al., The effect of post annealing temperature on grain size of indium-tin-oxide for optical and electrical properties improvement. Results in Physics., **13**,102159, 2019.

[35] Baía, I., et al., Performances exhibited by large area ITO layers produced by r.f. magnetron sputtering. Thin Solid Films.,**337(1)**, 171-175, 1999.

[36] Wang, W.-K., et al., Influence of Annealing Temperature on the Properties of ZnGa2O4 Thin Films by Magnetron Sputtering.. **9(12)**, 859, 2019.

[37] Lai, C.-m., K.-m. Lin, and S. Rosmaidah, Effect of annealing temperature on the quality of Al-doped ZnO thin films prepared by sol–gel method. Journal of Sol-Gel Science and Technology., 61(1), 249-257, 2012.

[38] Jun, M.C., et al., The microstructure of Al-doped ZnO thin films by a sol-gel dip-coating method., **13(6)**, 721-724, 2012.

[39] Rasool, S., et al., Effect of annealing on the physical properties of thermally evaporated In2S3 thin films. Current Applied Physics., **19(2)**, 108-113, 2019.

[40] Muchuweni, E., T.S. Sathiaraj, and H. Nyakotyo, Synthesis and characterization of zinc oxide thin films for optoelectronic applications. Heliyon., **3(4)**, e00285, 2017.

[41] Shinde, S.S., et al., Structural, optoelectronic, luminescence and thermal properties of Ga-doped zinc oxide thin films. Applied Surface Science., **258(24)**, 9969-9976, 2017.

[42] Mei-Zhen, G., et al., Effect of Annealing Conditions on Properties of Sol-Gel Derived Al-Doped ZnO Thin Films. Chinese Physics Letters., **26(8)**, 088105, 2009.

[43] Tong, H., et al., Effects of post-annealing on structural, optical and electrical properties of Al-doped ZnO thin films. Applied Surface Science., **257(11)**, 4906-4911, 2011.

[44] Sabeeh, S.H. and R.H. Jassam, The effect of annealing temperature and Al dopant on characterization of ZnO thin films prepared by sol-gel method. Results in Physics., 10: p. 212-216, 2018.

[45] Adam, A.M., et al., Characterization and optical properties of bismuth chalcogenide films prepared by pulsed laser deposition technique. Materials Science in Semiconductor Processing., **57**, 210-219, 2017.

[46] Behera, M., N.C. Mishra, and R. Naik, Thermal annealing induced evolution of Bi3Se2 topological phase from Bi/As2Se3 thin film: Structural, optical and morphological study. Physica B: Condensed Matter., 560, 51-59, 2019.

[47] Amer, M.I., S.H. Moustafa, and M. El-Hagary, Enhanced band structure, optoelectronic and magnetic properties of spray pyrolysis Ni-doped SnO2 nanostructured films. Materials Chemistry and Physics., 248, 122892, 2020.

[48] Fritzsche, H. and J.J.P.P. Tauc, New York,) p, Amorphous and liquid semiconductors., 254, 1974.

[49] Mott, N. and E.J.C. Davis, Oxford, Electronic processes in non-crystalline semiconductors., 220, 1979.

[50] El-Hagary, M., et al., Influences of Mn doping on the microstructural, semiconducting, and optoelectronic properties of HgO nanostructure films. Journal of the American Ceramic Society., 102(8), 4737-4747, 2019.

[51] Xu, Z., et al., Influence of thermal annealing on electrical and optical properties of indium tin oxide thin films. Materials Science in Semiconductor Processing., **26**, 588-592, 2014.

[52] Lee, J.H., et al., Grain-size effect on the electrical properties of nanocrystalline indium tin oxide thin films. Materials Science and Engineering: B., **199**, 37-41, 2015.